



In situ measurement of hydrogen concentration in steel using laser-induced breakdown spectroscopy (LIBS)

L. Quackatz¹ · A. Griesche¹ · J. Nietzke¹ · T. Kannengiesser^{1,2}

Received: 6 October 2023 / Accepted: 23 December 2023
© The Author(s) 2024

Abstract

The ISO 3690 standard “Determination of hydrogen content in arc weld metal” requires a thermal activation of the diffusible hydrogen in a piece of weld metal for the subsequent ex situ concentration measurement by carrier gas hot extraction CGHE or thermal desorption spectroscopy (TCD). Laser-induced breakdown spectroscopy (LIBS) offers a time and spatially resolved, almost non-destructive, in situ measurement of hydrogen at surfaces without sample preparation. We measured hydrogen in steels, which were charged either electrochemically or by high-pressure hydrogen gas, and compared the results. Further, the feasibility of quantitative hydrogen line scan measurements with LIBS was demonstrated by measuring hydrogen at water jet cut surfaces. The hydrogen concentrations measured with the help of LIBS were compared with CGHE measurements. It was observed that hydrogen can be reliably measured with LIBS for concentrations larger than 2 wt.-ppm. The maximum hydrogen concentration achieved using electrochemical charging was 85.1 ppm. The results show that LIBS is a promising technique for time- and spatially resolved measurements of hydrogen in steels.

Keywords LIBS · Hydrogen measurement · Welding · Stainless steel · Diffusible hydrogen

1 Introduction

During the welding of steels, critical combinations of diffusible hydrogen, hardened microstructure, and welding residual stresses can occur, leading to the formation of cold cracks in the welded joint's structure. For material damage caused by hydrogen, the two most accepted theories are

presented. Hydrogen enhanced decohesion (HEDE) [1, 2] and hydrogen enhanced localized plasticity (HELP) [3]. According to HEDE, hydrogen diffuses towards areas of high mechanical stress and strain. There, it reduces the bonding forces between metal atoms. HELP postulates that the hydrogen in the material accelerates the dislocation movements and reduces the yield point due to the improved slip processes in the material. The local deformation capacity is increased. If the local elongation capacity in the microstructure is reduced by the uptake of hydrogen and, in addition, overstressing occurs, hydrogen-assisted material damage can result. When hydrogen is taken up during operation or production, it can be transported either directly at the pickup location or into critical areas of the material, such as highly stressed areas or brittle microstructure areas.

The hydrogen can be absorbed into the material in different ways. One example is the diffusion of dissociated hydrogen from the plasma of the shielding gas during arc welding into the weld pool, where it remains after solidification [4–6]. Another possible path could be diffusion from the surface to the interior of the material due to corrosion processes [7]. The service life of steels can be affected by the uptake of hydrogen, leading to the degradation of mechanical properties and possibly to the formation of hydrogen-induced

Recommended for publication by Commission XII - Arc Welding Processes and Production Systems

✉ L. Quackatz
lukas.quackatz@bam.de
A. Griesche
axel.griesche@bam.de
J. Nietzke
jonathan.nietzke@bam.de
T. Kannengiesser
thomas.kannengiesser@bam.de

¹ Federal Institute for Materials Research and Testing, Unter den Eichen 87, 12205 Berlin, Germany

² Otto von Guericke University of Magdeburg, Institute of Materials and Joining Technology (IWF), Universitätsplatz 2, 39106 Magdeburg, Germany

cracking (HIC). Numerous research papers have thoroughly investigated various parameters affecting the susceptibility to hydrogen embrittlement. These parameters include hydrogen content, residual stresses, and deformation due to internal or external forces and microstructural features. All these influencing factors can cause a critical condition that eventually leads to hydrogen embrittlement [8–10]. HIC is often called cold cracking in welding technology and can lead to failure of the material or the component in service [11–13].

The diffusibility for hydrogen in austenitic stainless steels is in the order of 10^{-4} compared to ferritic steels. These steels have a decrease in ductility and can show brittle cracking during hydrogen charging [14]. If both the nickel concentration and the martensite content in the steel are increased, the susceptibility to hydrogen embrittlement increases due to changes in the crack growth mechanism. Martensite is considered to be a very susceptible microstructure for hydrogen embrittlement, which is why retained austenite is usually present in martensitic stainless steels to decelerate hydrogen embrittlement [15, 16]. The diffusibility of hydrogen in duplex stainless steels depends on the phase distribution due to the mixed matrix of austenite and ferrite. Investigations into hydrogen embrittlement in duplex steels can be found in [17, 18].

Several approaches exist to minimize the risk of HIC by limiting hydrogen uptake. Examples include reducing hydrogen uptake from electrochemical reactions by adding corrosion inhibitors or applying a surface coating that acts as a barrier to hydrogen diffusion. Furthermore, thermal degassing processes such as dehydrogenation heat treatment (DHT) can be used. In addition, various alloying elements such as vanadium, titanium, or boron can be used to improve the solubility of hydrogen in the material. They serve as so-called traps, where hydrogen collects and reduces the risk of damage to the material. In addition to the methods for controlling the hydrogen concentration in the material, there is considerable interest in precise hydrogen measurements in metals. This is particularly important for the evaluation of hydrogen uptake reactions or the success of heat treatment methods [19].

The international standard ISO 3690 [20] currently specifies how to measure diffusible hydrogen in deposited metal and fused weld metal. The *ex situ* concentration measurement is carried out with the help of carrier gas hot extraction (CGHE). In contrast, laser-induced breakdown spectroscopy (LIBS) would provide a temporally and spatially resolved, nearly non-destructive measurement of hydrogen on surfaces. Using a high-energy pulsed laser, the sample material is superficially heated, a micro-sized plasma is generated, and the material begins to vaporize. During the cooling of the plasma, element-specific electromagnetic radiation is emitted, which can be recorded wavelength-specifically

with the help of a spectrometer and which is analyzed with vendor's evaluation software [21, 22].

In previous studies, LIBS was successfully used for *in situ* measurement of chemical compositions during the welding of stainless steels. Main alloying elements such as Cr, Ni, and Mn could be measured both qualitatively and quantitatively [23–25]. Ball et al. [26] found in their investigations that it is possible to measure hydrogen using LIBS. They determined a detection limit of 20 wt.-ppm H for LIBS measurement in metals. They tested stainless steel, aluminum, copper, and titanium and introduced an external flow of H_2 gas. Hydrogen was supplied in gaseous form through a gas chamber and thus served as an external source of gaseous hydrogen. LIBS is particularly used for hydrogen detection in radioactive applications [27]. The advantage of LIBS is that a chemical analysis is possible without direct contact with a contaminated sample surface thus allowing applications, e.g., in the nuclear industry. Hydrogen and isotopes like deuterium were analyzed using LIBS by Fantoni et al. [28]. They coated Mo samples with W-Al and charged them with hydrogen to simulate contamination from nuclear applications. Marenkov et al. [29] conducted numerical calculations to estimate the relative error in LIBS measurements of H. They use tungsten as a base material with defined concentrations of hydrogen. They showed that as laser energy increases, the relative error of the measurements decreases. Xing et al. [30] investigated methods for quantitative measurement of hydrogen using LIBS in hydrogen storage materials. They analyzed hydrogen isotopes (Deuterium) in Ti and determined the hydrogen concentration in the materials using CGHE. They were able to achieve a relative error of 11%, which is still very high compared to a conventional CGHE (about 1–5%). Furthermore, hydrogen was measured in weld seams by Smith et al. [31]. They welded a low-alloyed steel in a GMAW process, with hydrogen-containing shielding gas. They performed LIBS measurements as a line scan perpendicular to the welding direction to determine the distribution in the WM and the HAZ. They observed that the hydrogen distribution in the weld seam can be measured reliably with LIBS, but they could not establish reproducibility in their applications for quantitative measurements. In general, it can be concluded that hydrogen measurements with LIBS are commonly used only in the nuclear industry [32].

Another application area that is highly relevant, especially for a possible extension of ISO 3690, is the use of handheld LIBS devices. These allow, for example, the on-site detection of various elements, on components already installed or in use. Noll et al. [33] provide an overview of current applications of handheld LIBS devices as well as new research and development projects in various industries. For applications that allow a low pulse energy and a small measuring distance (a few cm), the authors see a good opportunity for the use of miniaturized LIBS measurement devices.

Some studies show that with multivariate data analysis and appropriate software, a better analytical performance can be achieved than with comparable XRF handheld instruments [34, 35]. Afgan et al. [36] used a specially designed handheld LIBS device to determine the elements Si, Cr, Mn, Ni, Mo, V, C, and Cu quantitatively in high and low alloy steel. The accuracy of the LIBS results can be compared with the results of commercial XRF instruments already in industrial use. Pochon et al. [37] also used a handheld LIBS device in their study to detect gold occurrences in gold ore and gold alloys. The advantage here was that the LIBS device could be used directly on site, when mining the gold, and the samples did not have to be investigated in the laboratory. In some studies, hydrogen could be measured using a handheld LIBS device. For example, Garlea et al. [38] showed that they could reliably perform LIBS measurements on uranium samples containing defined hydrogen concentrations using a handheld device. They studied four samples, with hydrogen concentrations between 1.8 and 14 wt.-ppm and analyzed the atomic emission lines of H. In austenitic steels, Truschner et al. [39] measured hydrogen using handheld LIBS. They investigated the hydrogen embrittlement of an austenitic steel and analyzed the hydrogen concentration on the sample surface by handheld LIBS. The steel samples were either unloaded or electrochemically loaded. Their data sets showed a large scatter of concentrations, due to fluctuating laser energy. Also, the excitation energy of 6 mJ/pulse of the handheld device is very low and can cause scatter at low concentrations. However, they were able to find qualitative trends and a correlation with the LIBS intensities and concluded that this is a successful method to measure hydrogen in steels.

In this work, hydrogen in stainless steels is measured both qualitatively and quantitatively with LIBS. Experiments with time and spatially resolved measurements of hydrogen concentrations using LIBS were performed, and the total hydrogen concentration was measured using CGHE.

2 Materials and methods

2.1 Investigated materials and sample geometry

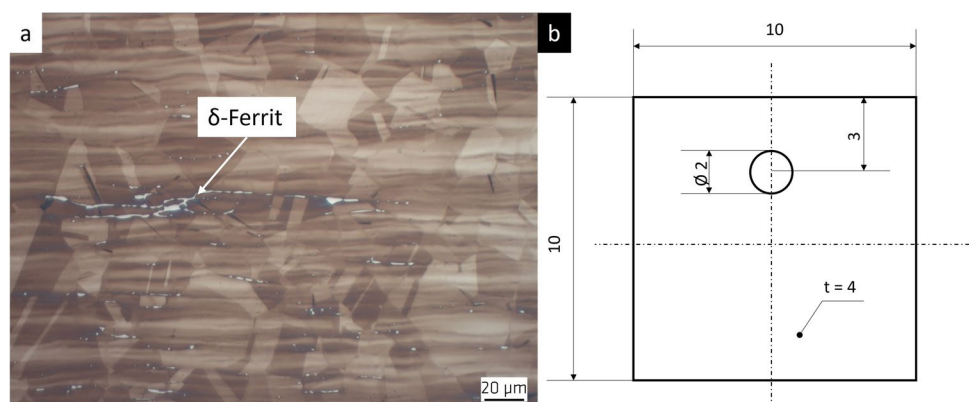
For these investigations, austenitic stainless steels of the grade EN 1.4301 were selected. In body-centered cubic (bcc) lattice, i.e., for ferritic and martensitic steels, hydrogen has a higher diffusion rate than in austenitic steels with face-centered cubic (fcc) lattice. This can be explained by the higher solubility of hydrogen in austenitic steels [40, 41]. Because of this lower diffusion rate and higher solubility of hydrogen in austenite than in ferrite, EN 1.4301 was chosen for the experiments. Table 1 shows the chemical composition, which was measured using optical emission spectroscopy (OES).

In addition, the microstructure was examined by preparing metallographic microsections of the base material. Figure 1a shows the microstructure of the used material EN 1.4301. The material was etched using Lichtenegger-Bloech I (LB I) etchant. A typical austenitic structure with a low volume fraction of δ -ferrite can be observed. Additionally, the hardness of the material was analyzed using Vickers hardness measurement (HV1). On average, the hardness of the material was $190 \text{ HV1} \pm 0.5$. Figure 1b illustrates the sample geometry used. This selected geometry has been

Table 1 Chemical composition of the material used (EN 1.4301), measured with OES

Grade (EN 10088-1)	Chemical composition (wt. %)						
	C	Si	Mn	Cr	Ni	Mo	Fe
1.4301	0.032	0.35	1.30	19.59	8.10	0.26	Bal.

Fig. 1 a Light microscope image of EN 1.4301. Ground, polished, and etched with LB I. b Technical drawing of the specimen. Dimensions in mm



established for electrochemical hydrogen charging and is therefore also used in these investigations.

2.2 Hydrogen charging and measurement

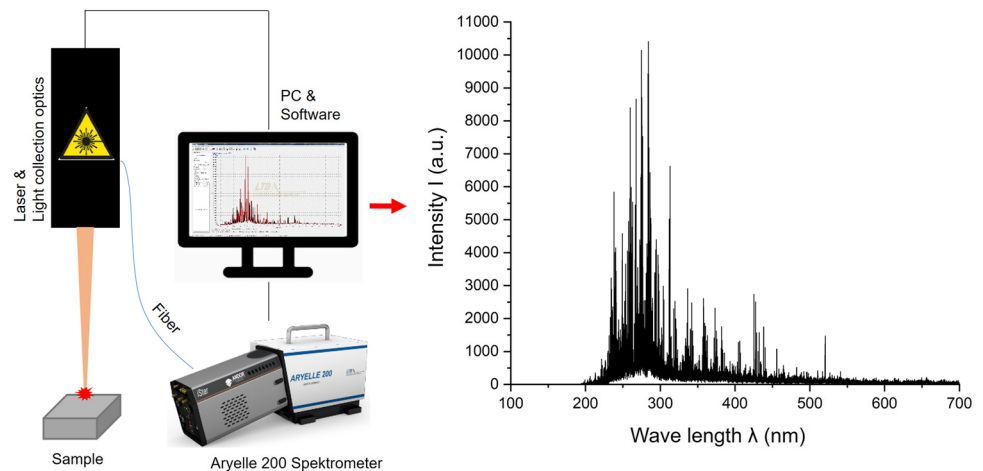
The hydrogen charging was performed using conventional cathodic charging in galvanostatic mode. This mode involved a constant current density provided by a galvanostat (Wenking TG 97 from Bank Elektronik in Germany). A 0.05 M H_2SO_4 (sulfuric acid) aqueous solution was used as the electrolyte. The sample under investigation served as the cathodic working electrode, while a Pt1800 electrode from SI Analytics, Germany, was used as the anodic counterpart. Further information on the electrochemical charging can be found in [42]. Prior to charging, each sample was ground with sanding paper type 600 and cleaned in an ultrasonic bath with acetone. The solution was additionally purged with argon to remove oxygen from the solution and prevent corrosion of the sample. The charging was performed at room temperature. One sample was charged at 50 °C using a heating plate controlled by a PT100 element for temperature control. The current density for each sample was 50 mA/cm². Table 3 provides the sample names and the parameters of the electrochemical charging. In addition, two more samples were charged with hydrogen using pressure gas charging to investigate a different charging method. The two samples were charged with different parameters. Autoclaves were used, which were evacuated before charging. Subsequently, they were flushed once with N_2 and three times with H_2 . One sample was heated to 200 °C and the other one to 150 °C. The heating was turned off 24 h prior to sample extraction. Following the charging, the samples were stored and transported in liquid nitrogen. The measurement of the concentration of diffusible hydrogen was conducted using a G8 Galileo analyzer from Bruker AXS and a coupled quadrupole mass spectrometer (MS) ESD100 from InProcess Instruments. This specific analyzer utilizes the carrier gas hot

extraction (CGHE) method. In this experimental approach, the sample was heated inside a glass tube using an infrared radiation-emitting furnace, IR07, which is part of the Galileo G8 system. By thermally activating the hydrogen present in the sample and employing a carrier gas stream of N_2 , the hydrogen was transported to the MS detection unit. Prior calibration of the system using different defined quantities of hydrogen allowed for precise adjustment for measuring minute amounts of hydrogen. Before measuring the hydrogen concentration, the sample was thawed in acetone at ambient temperature for approximately 60 s and subsequently dried in an N_2 gas stream for 60 s.

2.3 LIBS measurements

The LIBS system consists of a pulsed Nd:YAG laser with a wavelength of 1064 nm, a pulse rate of 15 Hz, and a maximum pulse energy of 200 mJ (Quantel CFR 200). The laser was synchronized using an Echelle spectrometer (Aryelle 200) from LTB Lasertechnik Berlin GmbH, which was connected to an Andor iStar ICCD camera from Oxford Instruments for maximum temporal resolution [43]. The experimental setup is depicted as a sketch in Fig. 2. A focusing lens (focal length: 300 mm) was used to focus the laser beam onto the sample surface. The electromagnetic radiation was then collected by an optical fiber (in the same system) with a focal length of 10 mm and directed into the spectrometer. In all experiments, a gate width of 40 μs and a delay time of 1 μs were used. These configurations have shown promise in previous experiments to obtain optimal LIBS intensities. Therefore, they are now also used to measure hydrogen in steel [23, 25]. For each spectrum acquisition, 15 laser pulses were accumulated. The LIBS spectra were recorded in the spectral range of 200–800 nm. The background noise in the acquired spectra was removed using the AirPls software [44]. The measurements were conducted in atmospheric conditions. To investigate the hydrogen concentration in

Fig. 2 Sketch of the experimental setup (left) and typical LIBS spectrum of a stainless steel (EN 1.4301) (right)



both the certified reference materials and the hydrogen-charged samples, LIBS measurements were performed on the surface of the samples (see Fig. 2). A high-energy laser was used to generate a microplasma on the surface of the samples. During the cooling of the plasma, element-specific light is released, which was recorded by the spectrometer. In this publication, only the H α wavelength at 656.27 nm was considered [45]. The same measurement setup is used to generate depth profiles. However, multiple LIBS measurements (up to 10,000 measurements) are now performed in the same location, on the surface of the sample to obtain information about the hydrogen distribution to the depth of the sample. The depth was recorded using a micrometer after every 10th LIBS measurement.

3 Results and discussion

3.1 Reference materials

Certified reference materials are materials with known, defined concentrations of the element under investigation. They often serve as a comparative measurand in a measurement procedure. The reference materials are used to calibrate CGHE systems so that hydrogen can be measured reliably. The reference samples were measured as shown in Fig. 2 so that LIBS measurements could be performed on the surface of the reference samples. Using the known hydrogen concentrations of the reference materials, these could be plotted vs. the LIBS intensities. The reference materials were obtained from the Federal Institute for Materials Research and Testing in Berlin (BAM H1) [46] and from LECO (LECO 502-928 and LECO 502-963) [47]. The samples were austenitic steel, charged with hydrogen. The sample designations along with their respective hydrogen concentrations are presented in Table 2.

The measurement was conducted on the surface of the samples. Figure 3 displays the results of the initial hydrogen measurements using LIBS on reference materials. Since the materials are steel, the LIBS intensities are normalized to an iron line Fe I at 373.49 nm. This one was chosen because it had the highest intensities in the spectra and provided good visibility. The error bars result from six

Table 2 Certified reference materials with associated hydrogen concentrations from the manufacturers

Sample name (-)	Hydrogen concentration (wt.-ppm)
BAM H1	1.0
LECO 502-928	2.6
LECO 502-963	6.9

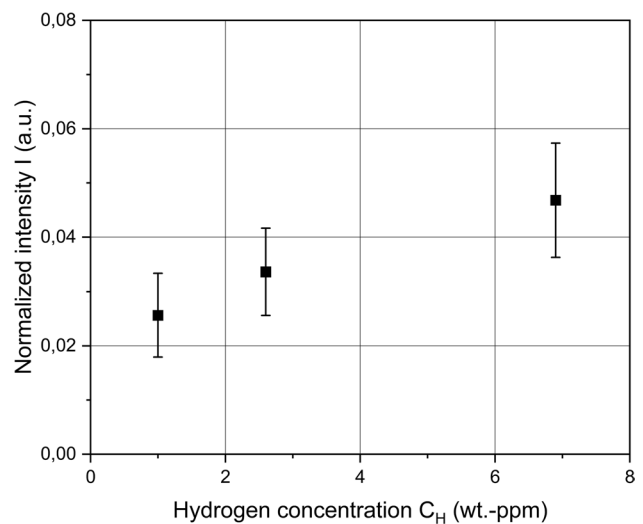


Fig. 3 LIBS intensities (Hydrogen line H α 656.27 nm) plotted vs. hydrogen concentrations of the reference materials. The error bars represent the standard deviation and result from the measurement of six different measurements of the same reference material

different measurements of the same reference sample. The results demonstrate that the LIBS intensities increase with increasing hydrogen concentration. Consequently, the results obtained with LIBS are valid. Below the given hydrogen concentrations, the qualitative determination is not possible, because there, the detection limit of the spectroscopic measuring technique LIBS is reached. A functional connection with the other measuring points is therefore not meaningful. It should be considered that the surface roughness has a great influence on the hydrogen LIBS signal [48]. However, the reference materials did not have uniform surface roughness. Therefore, all loaded samples were ground with sandpaper and a reproducible surface could be ensured. In a next step, this correlation of LIBS intensities and hydrogen concentrations will be used to generate a calibration curve.

3.2 Electrochemical charging and gas charging

After the samples were charged electrochemically, they were examined using LIBS and CGHE to determine the total concentration of hydrogen. Two samples were charged in parallel with the same parameters, allowing for comparable samples to create a calibration model for quantitative measurements and compare the measurement methods LIBS and CGHE. The measured hydrogen concentrations using CGHE are presented in Table 3.

LIBS measurements were also performed on the surface of the samples. Figure 4 shows the LIBS intensities of samples charged electrochemically. The hydrogen concentration from CGHE is plotted on the x -axis. The error bars represent the standard deviation from six different measurements

Table 3 Total hydrogen concentrations of the charged samples. These were determined with CGHE

Electrochemically charged samples	
Charging current density (mA/cm ²)/time (h)	Hydrogen concentration (wt.-ppm)
Reference	2.0
50/168	3.7
50/168	3.9
50/168	4.2
50/168	4.9
50/168	17.2
50/576 at 50 °C	18.6
50/192	28.1
50/576	85.1
Pressure gas charged samples	
Temperature (°C)/pressure (bar)	Hydrogen concentration (wt.-ppm)
200/200	34.2
150/1000	51.7

of the same sample. It is evident that an increase in LIBS intensities is observed with increasing hydrogen concentration, allowing for the creation of a calibration curve. Starting from the reference sample without hydrogen charging ($C_H = 2.0$ wt.-ppm), the calibration curve can be generated. The curve is not placed through the origin due to a measurement-specific y-axis shift. This shift is dependent on the measuring conditions and is determined by different parameters. For example by different absorption and evaporation characteristics of the surface, the particle emission as well as by deviations in the standardization and the atmosphere. As an alternative to calibration with certified reference materials, the calibration-free LIBS (CF-LIBS) method can be used [49]. CF-LIBS for hydrogen measurements was discussed by Almaviva et al. [50]. Figure 4b presents a depth profile of the sample with $C_H = 4.9$ wt.-ppm. Using the calibration curve from 4a, quantitative values could be plotted. The fit curve is a polynomial and serves as a guide to the eye. It is intended

to reflect the course of the measured hydrogen concentrations. The hydrogen concentration decreases steeply and stabilizes at a minimum of approximately 1.5 wt.-ppm. The distribution of hydrogen is predominantly surface-oriented, which is reasonable considering that hydrogen diffuses from the surface into the interior of the material during charging. The hydrogen concentration does not drop down to zero because even in the uncharged base metal a small amount of hydrogen is present ($C_H = 2.0$ wt.-ppm), measured by LIBS. However, some factors should be considered for the depth profiles: The laser applies heat energy multiple times to the same spot, leading to an increase in diffusion capability and potentially distorting the hydrogen concentration. Additionally, initially, there may be a higher water content on the surface due to storage in liquid nitrogen. Nevertheless, the measurement results are meaningful and warrant further investigation.

In addition to the electrochemically charged samples, two samples were also charged with hydrogen via pressurized gas. Figure 5 presents the depth profiles of these samples. The calibration curve derived from the electrochemically charged samples was used to obtain quantitative values of the hydrogen concentration in the samples. The fit curve is a polynomial and serves as a guide to the eye. It is intended to reflect the course of the measured hydrogen concentrations. Remarkably, the decrease in hydrogen concentration with depth in the material is less pronounced in these results. This is likely due to a higher overall hydrogen concentration (see Table 3) present in the material. Furthermore, the duration and method of charging also influence the distribution of hydrogen within the material. The hydrogen concentration does not drop to 0 wt.-ppm since hydrogen is still contained in the uncharged base metal.

To investigate the distribution of hydrogen within the material, one sample ($C_H = 17.2$ wt.-ppm) was cut in the middle, and a line scan was performed using LIBS. The line scan was conducted on the cut surface towards both ends of the sample, with a step size of 0.5 mm. Waterjet cutting was used to minimize the heat input into the specimen.

Fig. 4 **a** LIBS intensities plotted vs. hydrogen concentrations after electrochemical charging. The error bars result from the measurement of six different measurements of the same sample. **b** Depth profile of a sample after electrochemical charging. $C_H = 4.9$ wt.-ppm. Using the calibration curve from **a**, the concentrations could also be plotted quantitatively. The fit curve is a guide to the eye

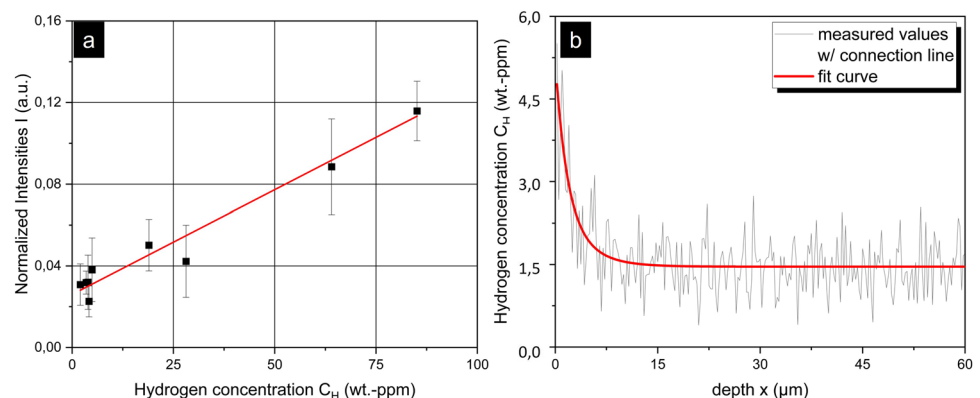


Fig. 5 **a** Depth profile of the pressure gas charged sample, 200 bar, 200 °C; **b** depth profile of the pressure gas charged sample, 1000 bar, 150 °C

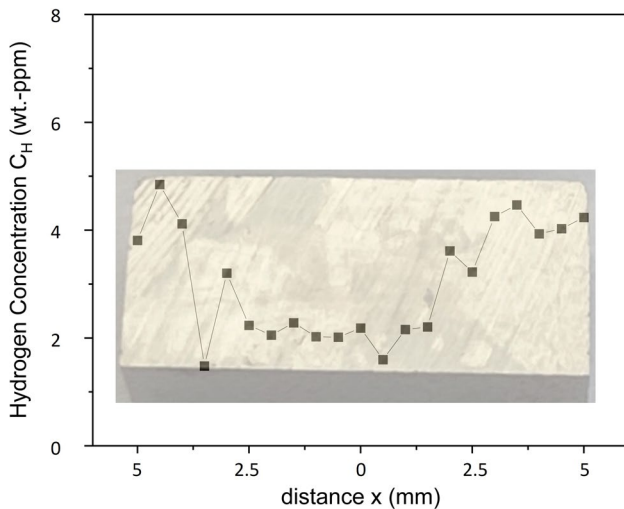
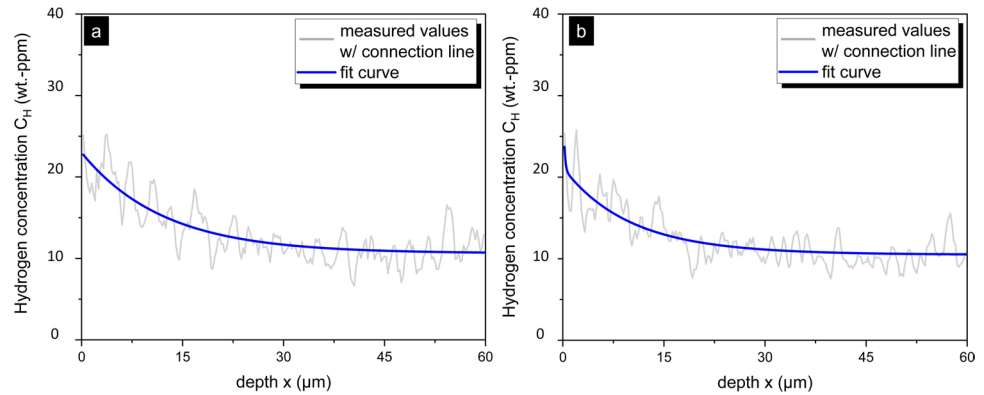


Fig. 6 LIBS line scan of water jet cut sample, squares represent measuring points with connecting line to guide the eye; $C_H = 18.6$ wt.-ppm, charging current density: 50 mA, time: 576 h at 50 °C. The course of the hydrogen concentrations vs. the cross-section. $X=0$ represents the center of the sample

Immediately after charging, the sample was stored in liquid nitrogen, taken to waterjet cutting, and then immediately placed back in liquid nitrogen until subsequent testing. Despite the cutting method chosen, which introduces a small amount of heat into the material and does not strongly activate the hydrogen, it should be noted that the sample was exposed to the atmosphere for some time, allowing the hydrogen to diffuse out. The results are shown in Fig. 6. They show a clear trend, with hydrogen concentration accumulating at the edges of the sample and decreasing towards the center. This is consistent with the behavior of hydrogen initially diffusing from the surfaces and gradually moving deeper into the material over time. It should also be considered that water may remain on the surface of the sample after removal from liquid nitrogen. In general, LIBS proves to be suitable for measuring hydrogen in steel. However, further investigations should be conducted to validate the results.

Furthermore, the experimental conditions should be varied. In other publications, it was found that the LIBS signal of the hydrogen line $H\alpha$ was improved, by measurements in helium atmosphere and lower ambient pressure [51, 52]. To our knowledge, no publication currently exists on the quantitative measurement of hydrogen in steel or in weld seams with LIBS, so there is a great demand for research and to expand the literature. Individual publications show qualitative measurements, but these have not been continued [31].

4 Conclusion

The objective of this work was to verify the feasibility of measuring quantitatively hydrogen in steel using LIBS. The advantage of LIBS is its ability to perform fast, temporally, and spatially resolved measurements on the surface of metals. Commercially available certified reference materials were examined to evaluate the measurement technique. Furthermore, austenitic steel samples were charged electrochemically and with hydrogen pressure gas. With the help of LIBS measurements, a calibration model could be established, and quantitative measurements were realized. The total hydrogen concentration was determined by CGHE. It was found that LIBS measurements provided satisfying results even at low hydrogen concentrations and showed a trend with increasing concentrations. By combining surface measurements with total volume concentrations obtained from CGHE, a calibration curve can be generated that allows quantitative measurements. This approach was used in depth profiling to visualize the hydrogen diffusion in the steel. Spatially resolved measurements were made on a water jet cut sample. In the future, the measurement technique for hydrogen in steels and welds should be further optimized. For example, experiments under a vacuum and inert gas atmosphere could help to maximize the LIBS intensities for hydrogen. We have successfully demonstrated that it is possible to determine spatially resolved hydrogen concentrations quantitatively using LIBS. This method can

be applied to welds to visualize local hydrogen concentrations and minimize in situ welding hazards. It is a valuable complement to CGHE.

Acknowledgements Mareike Kirstein and Marina Marten are thanked for their assistance with metallographic preparation. The authors would like to thank Lasertechnik Berlin GmbH (LTB) for supporting the LIBS measurements.

Funding Open Access funding enabled and organized by Projekt DEAL. This work was funded by the Deutsche Forschungsgemeinschaft (DFG, German Research Foundation) – 442001176.

Declarations

Competing interests The authors declare no competing interests.

Open Access This article is licensed under a Creative Commons Attribution 4.0 International License, which permits use, sharing, adaptation, distribution and reproduction in any medium or format, as long as you give appropriate credit to the original author(s) and the source, provide a link to the Creative Commons licence, and indicate if changes were made. The images or other third party material in this article are included in the article's Creative Commons licence, unless indicated otherwise in a credit line to the material. If material is not included in the article's Creative Commons licence and your intended use is not permitted by statutory regulation or exceeds the permitted use, you will need to obtain permission directly from the copyright holder. To view a copy of this licence, visit <http://creativecommons.org/licenses/by/4.0/>.

References

1. Troiano AR (1960) The role of hydrogen and other interstitials in the mechanical behavior of metals. *Trans Am Soc Met* 52:54–80
2. Oriani R (1972) A mechanistic theory of hydrogen embrittlement of steels. *Ber Bunsenges Phys Chem* 76(8):848–857
3. Birnbaum HK, Sofronis P (1994) Hydrogen-enhanced localized plasticity—a mechanism for hydrogen-related fracture. *Mater Sci Eng A* 176(1–2):191–202
4. Mundra K, Blackburn JM, DebRoy T (1997) Absorption and transport of hydrogen during gas metal arc welding of low alloy steel. *Sci Technol Weld Join* 2(4):174–184. <https://doi.org/10.1179/stw.1997.2.4.174>
5. Kasuya T, Hashiba Y, Ohkita S, Fuji M (2001) Hydrogen distribution in multipass submerged arc weld metals. *Sci Technol Weld Join* 6(4):261–266
6. Patchett B, Yarmuch M (2010) Hydrocarbon contamination and diffusible hydrogen levels in shielded metal arc weld deposits. *Weld J* 89:262–265
7. Iyer RN, Pickering HW (1990) Mechanism and kinetics of electrochemical hydrogen entry and degradation of metallic systems. *Annu Rev Mater Sci* 20(1):299–338
8. Akiyama E (2012) Evaluation of delayed fracture property of high strength bolt steels. *ISIJ Int* 52(2):307–315
9. Rozenak P, Robertson I, Birnbaum H (1990) HVEM studies of the effects of hydrogen on the deformation and fracture of AISI type 316 austenitic stainless steel. *Acta Metall Mater* 38(11):2031–2040
10. Luppó M, Ovejero-García J (1991) The influence of microstructure on the trapping and diffusion of hydrogen in a low carbon steel. *Corros Sci* 32(10):1125–1136
11. Husemann R, Devrient S, Kilian R (2012) Cracking mechanism in high temperature water-T24 Root cause analysis program. In: 38th VDI-Jahrestagung Schadensanalyse in Kraftwerken. VDI-Wissensforum, Düsseldorf, pp 87–103
12. Steppan E, Mantzke P, Steffens BR, Rhode M, Kannengiesser T (2017) Thermal desorption analysis for hydrogen trapping in microalloyed high-strength steels. *Weld World* 61(4):637–648. <https://doi.org/10.1007/s40194-017-0451-z>
13. Chakraborty G, Rejeesh R, Ramana OV, Albert SK (2020) Evaluation of hydrogen-assisted cracking susceptibility in modified 9cr-1mo steel welds. *Weld World* 64(1):115–122. <https://doi.org/10.1007/s40194-019-00812-2>
14. Murakami Y, Kanezaki T, Mine Y et al (2008) Hydrogen embrittlement mechanism in fatigue of austenitic stainless steels. *Metall Mater Trans A* 39:1327–1339. <https://doi.org/10.1007/s11661-008-9506-5>
15. Brück S et al (2018) Hydrogen embrittlement mechanism in fatigue behavior of austenitic and martensitic stainless steels. *Metals* 8(5):339
16. Fan YH, Zhang B, Yi HL, Hao GS, Sun YY, Wang JQ, Han E-H, Ke W (2017) The role of reversed austenite in hydrogen embrittlement fracture of S41500 martensitic stainless steel. *Acta Mater* 139:188–195, ISSN 1359-6454. <https://doi.org/10.1016/j.actamat.2017.08.011>
17. Boellinghaus T et al (1996) Scatterbands for hydrogen diffusion coefficients in steels having a ferritic or martensitic microstructure and steels having an austenitic microstructure at room temperature. *Weld World/Le Soudage dans le Monde* 1(37):16–23
18. Turnbull A, Hutchings R (1994) Analysis of hydrogen atom transport in a two-phase alloy. *Mater Sci Eng A* 177(1–2):161–171
19. Salmi S, Rhode M, Jüttner S, Zinke M (2015) Hydrogen determination in 22MnB5 steel grade by use of carrier gas hot extraction technique. *Weld World* 59(1):137–144. <https://doi.org/10.1007/s40194-014-0186-z>
20. DIN EN ISO 6520 (2007). Schweißen und verwandte Prozesse. Einteilung von geometrischen Unregelmäßigkeiten an metallischen Werkstoffen - Teil 1: Schmelzschweißen
21. Noll R (2012) Laser-induced breakdown spectroscopy fundamentals and applications. Springer (in eng), Berlin
22. Cremers DA, Radziemski LJ (2006) Handbook of laser-induced breakdown spectroscopy, 2nd edn. Wiley (in eng), Chichester
23. Quackatz L, Griesche A, Kannengiesser T (2022) In situ investigation of chemical composition during TIG welding in duplex stainless steels using Laser-Induced Breakdown Spectroscopy (LIBS). *Forces Mech* 6:100063. <https://doi.org/10.1016/j.finmec.2021.100063>
24. Quackatz L, Griesche A, Kannengiesser T (2022) Spatially resolved EDS, XRF and LIBS measurements of the chemical composition of duplex stainless steel welds: a comparison of methods. *Spectrochim Acta B At Spectrosc* 193:106439. <https://doi.org/10.1016/j.sab.2022.106439>
25. Quackatz L, Griesche A, Kannengiesser T (2023) Rapid solidification during welding of duplex stainless steels – in situ measurement of the chemical concentration by laser-induced breakdown spectroscopy (LIBS). *IOP Conf Ser: Mater Sci Eng* 1274(1):012018. <https://doi.org/10.1088/1757-899X/1274/1/012018>
26. Ball AJ, Hohreiter V, Hahn DW (2005) Hydrogen leak detection using laser-induced breakdown spectroscopy. *Appl Spectrosc* 59(3):348–353. <https://doi.org/10.1366/0003702053585282>
27. Kautz EJ et al (2021). Detection of hydrogen isotopes in Zircaloy-4 via femtosecond LIBS. *J Anal At Spectrom*. <https://doi.org/10.1039/D1JA00034A>
28. Fantoni R et al (2017) Hydrogen isotope detection in metal matrix using double-pulse laser-induced breakdown-spectroscopy.

- Spectrochim Acta B At Spectrosc 129:8–13. <https://doi.org/10.1016/j.sab.2016.12.008>
29. Marenkov ED, Tsygvintsev IP, Gasparyan YM, Stepanenko AA (2021, ARTN 101029) Assessment of laser induced breakdown spectroscopy accuracy for determination of hydrogen accumulation in tungsten. Nucl Mater Energy 28:101029. <https://doi.org/10.1016/j.nme.2021.101029>
 30. Xing Y et al (2022) Quantitative analysis of hydrogen isotopes in hydrogen storage material using laser-induced breakdown spectroscopy. Nucl Mater Energy 31:101204. <https://doi.org/10.1016/j.nme.2022.101204>
 31. Smith R, Landis G, Maroef I, Olson D, Wildeman T (2001) The determination of hydrogen distribution in high-strength steel weldments Part 1: laser ablation methods. Weld J-New York 80(5):115-s
 32. Weiss Z (2021) Analysis of hydrogen in inorganic materials and coatings: a critical review. Hydrogen 2(2):225–245 [Online]. Available: <https://www.mdpi.com/2673-4141/2/2/12>
 33. Noll R, Fricke-Begemann C, Connemann S, Meinhardt C, Sturm V (2018) LIBS analyses for industrial applications—an overview of developments from 2014 to 2018. J Anal At Spectrom 33(6):945–956
 34. Noll R et al (2014) Laser-induced breakdown spectroscopy expands into industrial applications. Spectrochim Acta B At Spectrosc 93:41–51
 35. Gaft M, Nagli L, Groisman Y, Barishnikov A (2014) Industrial online raw materials analyzer based on laser-induced breakdown spectroscopy. Appl Spectrosc 68(9):1004–1015
 36. Afgan MS, Hou Z, Wang Z (2017) Quantitative analysis of common elements in steel using a handheld μ -LIBS instrument. J Anal At Spectrom 32(10):1905–1915
 37. Pochon A, Desaulty A-M, Bailly L (2020) Handheld laser-induced breakdown spectroscopy (LIBS) as a fast and easy method to trace gold. J Anal At Spectrom 35(2):254–264
 38. Garlea E, Bennett B, Martin MZ, Bridges R, Powell G, Leckey JH (2019) Novel use of a hand-held laser induced breakdown spectroscopy instrument to monitor hydride corrosion in uranium. Spectrochim Acta B At Spectrosc 159:105651
 39. Truschner M, Kroll R, Eichinger M, Keplinger A, Engelberg DL, Mori G (2023) Hydrogen embrittlement characteristics in cold-drawn high-strength stainless steel wires. Corros Sci 216:111109
 40. Das T, Legrand E, Brahimi SV, Song J, Yue S (2020) Evaluation of material susceptibility to hydrogen embrittlement (HE): an approach based on experimental and finite element (FE) analyses. Eng Fract Mech 224:106714
 41. Jeklih, Absorpcija In Difuzija Vodika V (2000) Absorption and diffusion of hydrogen in steels. Materiali in tehnologije 34(6):331
 42. Rhode M, (2016) “Hydrogen diffusion and effect on degradation in welded microstructures of creep-resistant low-alloyed steels,” 148, Bundesanstalt für Materialforschung und -prüfung (BAM), Berlin, PhD Thesis.
 43. Mueller M, Gornushkin IB, Florek S, Mory D, Panne U (2007) Approach to detection in laser-induced breakdown spectroscopy. Anal Chem 79(12):4419–4426. <https://doi.org/10.1021/ac0621470>
 44. Zhang Z-M, Chen S, Liang Y-Z (2010) Baseline correction using adaptive iteratively reweighted penalized least squares. Analyst 135(5):1138–1146
 45. NIST Technology (2003) NIST atomic spectra database lines form. https://physics.nist.gov/PhysRefData/ASD/lines_form.html. Accessed 01.03.2023
 46. Bundesanstalt für Materialforschung und -prüfung. “BAM Webshop.” Bundesanstalt für Materialforschung und -prüfung. https://webshop.bam.de/webshop_de/referenzmaterialien/eisen-stahl/stahl-mit-zertifiziertem-sauer-stick-und-wasserstoffgehalt/zrm-stahl-h1-1350.html. Accessed 2023
 47. Leco (2023) Reference Materials and Standards Catalog. <https://knowledge.leco.com/component/edocman/reference-materials-and-standards-catalog-209-296?tmpl=component&Itemid=32>
 48. Rapin W et al (2017) Roughness effects on the hydrogen signal in laser-induced breakdown spectroscopy. Spectrochim Acta B At Spectrosc 137:13–22
 49. Demidov A et al (2016) Monte Carlo standardless approach for laser induced breakdown spectroscopy based on massive parallel graphic processing unit computing. Spectrochim Acta B 125:97–102 [Online]. Available: <https://opus4.kobv.de/opus4-bam/frontdoor/index/index/docId/38489>
 50. Almaviva S, Caneve L, Colao F, Maddaluno G, Fantoni R (2021) Accessory laboratory measurements to support quantification of hydrogen isotopes by in-situ LIBS from a robotic arm inside a fusion vessel. Spectrochim Acta B At Spectrosc 181:106230. <https://doi.org/10.1016/j.sab.2021.106230>
 51. Pardede M et al (2018) H–D analysis employing energy transfer from metastable excited-state He in double-pulse LIBS with low-pressure He gas. Anal Chem 91(2):1571–1577
 52. Kurniawan KH et al (2006) Quantitative analysis of deuterium using laser-induced plasma at low pressure of helium. Anal Chem 78(16):5768–5773

Publisher's Note Springer Nature remains neutral with regard to jurisdictional claims in published maps and institutional affiliations.